Computer Fraud and Security

ISSN (online): 1873-7056

Emergence of Rich Patterns in a Discrete System with Migration and Diffusion

Jie Gao[1*], Jincheng Zheng[1], Chaofan Hu[1]

[1]Research Center for Engineering Ecology and Nonlinear Science, North China Electric Power University, Beijing 102206, P.R. China

* Corresponding author

E-mail: 120222209089@ncepu.edu.cn

Abstract

This study employs the pattern formation of a discrete system with migration and diffusion. By analyzing the stability of fixed points and flip and Neimark-Sacker bifurcations, we demonstrate the non-spatial form of the system can generate complex dynamical behaviors, including periodic, quasiperiodic and chaotic orbits. Numerical simulations reveal the emergence of rich patterns which show different ways of transitions, especially on the routes to chaos with the variation of bifurcation parameter. We find the migration in the discrete system enhances spatial coupling and reshapes pattern stability. This work connects bifurcation with spatiotemporal dynamics, revealing how migration-diffusion interaction drives pattern self-organization.

Keywords: Bifurcation; Pattern; Discrete system; Coupled map lattice; Chaos

1. Introduction

The development of mathematical models has significantly advanced our understanding of pattern formation in spatiotemporal systems [1, 2]. Until recently, reaction-diffusion models remained the most mainstream theoretical framework [3–5]. Reaction-diffusion models reflect two fundamental features: the reaction between system variables and the diffusion of these variables in space [6]. With the development of reaction-diffusion models, researchers have further incorporated another movement—migration—to explore the self-organization of patterns. Studies have found that the occurrence of migration significantly influences pattern formation, leading to the emergence of traveling waves [7, 8].

Building on reaction-diffusion models, the coupled map lattice (CML), which features discrete spatiotemporal properties and continuous variables, has been developed to explore the spatiotemporal dynamics [9, 10]. With the application of CML, researchers have uncovered new insights into the nonlinear characteristics of discrete systems [11]. Comparisons between reaction-diffusion model and corresponding CML demonstrated that CML can describe a broader range of spatiotemporal dynamics [6, 12]. Through the nonlinear mechanisms of CML, a deeper understanding of the spatiotemporal complexity of discrete systems has been achieved [1-2, 5-6, 9, 12].

In this research, we investigate the pattern formation in the spatiotemporally discrete predator-prey with diffusion and migration which is described by a three-chain CML,

$$u'_{(i,j,m)} = u_{(i,j,m)} + \frac{\tau}{l} C_1 \Gamma_d u_{(i,j,m)},\ v'_{(i,j,m)} = v_{(i,j,m)} + \frac{\tau}{l} C_2 \Gamma_d v_{(i,j,m)}, \tag{1a}$$

$$u''_{(i,j,m)} = u'_{(i,j,m)} + \frac{\tau}{l^2} D_1 \Delta_d u'_{(i,j,m)},\ v''_{(i,j,m)} = v'_{(i,j,m)} + \frac{\tau}{l^2} D_2 \Delta_d v'_{(i,j,m)}, \tag{1b}$$

$$u_{(i,j,m+1)} = f_1\left(u''_{(i,j,m)}, v''_{(i,j,m)}\right),\ v_{(i,j,m+1)} = g_1\left(u''_{(i,j,m)}, v''_{(i,j,m)}\right), \tag{1c}$$

where $u_{(i,j,m)}$ and $v_{(i,j,m)}$ $(i, j \in N)$ represent the prey density and the predator density in the (i, j) site at iteration m; $u'_{(i,j,m)}$, $v'_{(i,j,m)}$, and $u''_{(i,j,m)}$, $v''_{(i,j,m)}$ are intermediate states after the stages of migration and diffusion, respectively; parameters τ and l describe the temporal and spatial scales; D_1 and D_2 are prey and predator diffusion coefficients, and C_1 and C_2 are the migration coefficients; and

$$\Gamma_d\psi_{(i,j,m)} = \psi_{(i-1,j,m)} - \psi_{(i,j,m)}, \tag{2a}$$

$$\Delta_d\psi_{(i,j,m)} = \psi_{(i+1,j,m)} + \psi_{(i-1,j,m)} + \psi_{(i,j+1,m)} + \psi_{(i,j-1,m)} - 4\psi_{(i,j,m)}, \tag{2b}$$

$$f_1(u,v) = u + \tau\left(R\left(1-\frac{u}{S}\right)u - \frac{Suv}{v+Su}\right),\ g_1(u,v) = v + \tau\left(\frac{Suv}{v+Su} - Qv\right), \tag{2c}$$

in which symbol ψ represents the variable of either u or v; R, S and Q are nondimensionalized parameters of the ratio-dependent predator-prey system, and parameters R and Q can be regarded to represent the prey growth rate and the predator mortality rate.

2. System dynamical characteristics

To explore the pattern formation of system (1), its dynamical characteristics should be understood firstly. Via stability analysis and bifurcation analysis on the system, we can obtain the results for the fixed points, Turing instability, flip and Neimark-Sacker bifurcations. For the calculations, one can refer to the literature [9, 12]. The system (1) has two fixed points,

$$(u_1, v_1) = (S, 0), \tag{3a}$$

$$(u_2, v_2) = \left(\frac{S(R+S(Q-1))}{R}, \frac{S^2(1-Q)(R+S(Q-1))}{QR}\right),\ 1-R/S < Q < 1, \tag{3b}$$

and the stability of the two fixed points can be described as the following:

(1) The fixed point (u_1, v_1) is always unstable if (u_2, v_2) exists in the system;

(2) The fixed point (u_2, v_2) is stable if $-p < 1 + q$, $-p > -1 - q$, $q < 1$, where $p = -2 + \tau R - \tau(Q-1)\big(Q - S(Q+1)\big)$, $q = 1 - \tau(\tau Q(Q-1)+1)R - \tau^2 SQ(Q-1)^2 + \tau(Q-1)\big(Q - S(Q+1)\big)$.

The occurrence conditions for Turing instability can be described as

$$L = \max_{\bar{\imath},\bar{\jmath}}\left\{max\left(\left|\bar{\lambda}_+(\bar{\imath},\bar{\jmath})\right|, \left|\bar{\lambda}_-\bar{\imath},\bar{\jmath}\right|\right)\right\} > 1. \tag{4}$$

where $\bar{\lambda}_\pm(\bar{\imath},\bar{\jmath}) = \frac{1}{2}\left((A_{11}+A_{12}) \pm \sqrt{(A_{11}-A_{12})^2 + 4A_{12}A_{21}}\right)$ and A_{ij} is the elements of the Jacobian matrix associated to the spatiotemporal system (1).

The non-spatial system of (1) undergoes flip bifurcation at (u_2, v_2) if the following conditions are satisfied: (1) $R^* = -S(Q-1) + \frac{4+2\tau Q(Q-1)(1-S)}{\tau^2 Q(Q-1)+2\tau}$; (2) $\tau R^* - \tau(Q-1)\big(Q - S(Q+1)\big) \neq 2, 4$; (3) $\eta_1 = \mu_3 \neq 0$, and $\eta_2 = \mu_6 + \mu_1^2 \neq 0$. Moreover, if $\eta_2 > 0$, the period-2 points bifurcating from (u_2, v_2) are stable; if $\eta_2 < 0$, the bifurcating period-2 points are unstable. In the above conditions, the terms μ_1, μ_3, and μ_6 can be described as $\mu_1 = \tilde{f}_{1200}$, $\mu_3 = \tilde{f}_{1110}$, $\mu_6 = \tilde{f}_{1300} + e_1\tilde{f}_{1101}$, and the detailed calculations of these terms can be seen in [9, 12]. Simultaneously, the non-spatial system of (1) can also undergo a Neimark-Sacker bifurcation at the fixed point (u_2, v_2), and the bifurcation conditions can also be calculated using the method as described in previous approach [9, 12].

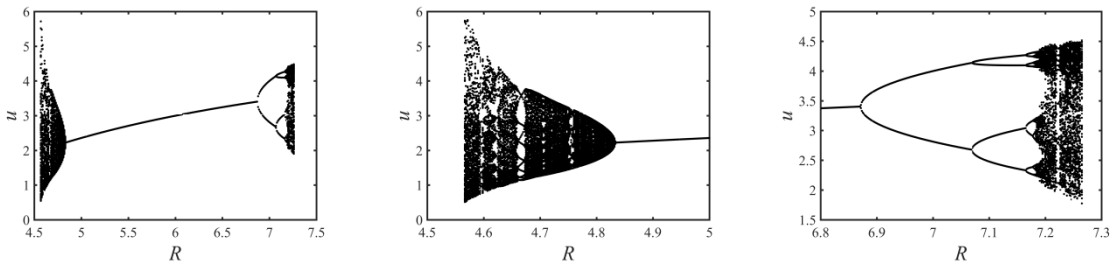

(a) 4.5-7.5 (b) 4.5-5.0 (c) 6.8-7.3

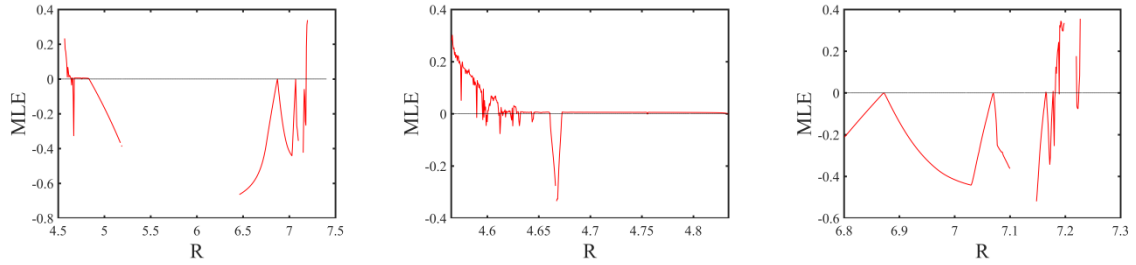

(d) 4.5-7.5 (e) 4.565-4.834 (f) 6.8-7.3

Fig. 1 Bifurcation diagram with the variation of parameter R the corresponding maximum Lyapunov exponent diagram.

Fig. 1a-1c shows the occurrence of Neimark-sacker bifurcation and flip bifurcation occur with the increase of parameter R. Fig. 1d-1f exhibits the maximum Lyapunov exponent diagrams corresponding, suggesting that chaotic behavior can take place on the routes to chaos induced by both Neimark-Sacker bifurcation and flip bifurcation. To be more accurate, system begins entering chaos from Neimark-Sacker bifurcation at $R = 4.65$, and $R = 7.2$ for flip bifurcation.

3. Pattern formation simulations

Numerical simulations are performed to demonstrate the pattern formation in a space with 200×200 grid cells. A group of feasible parameter values are provided in Table 1. The initial conditions for the pattern simulations are set as perturbing (u_2, v_2) using small random spatially heterogeneous perturbations. It should be noticed that the migration direction is set as from up to down in all pattern graphs.

Table 1. Parameter values provided for the pattern simulations of Figs. 2-4.

Parameter	R	Q	S	τ	δ	D_1	D_2	C_1	C_2
Fig. 2a	0.47	0.1	1	0.05	0.5	0.1	1	0	0
Fig. 2b	0.48	0.1	1	0.05	0.5	0.1	1	0	0
Fig. 2c	0.5	0.1	1	0.05	0.5	0.1	1	0	0
Fig. 2d	0.52	0.1	1	0.05	0.5	0.1	1	0	0
Fig. 2e	0.54	0.1	1	0.05	0.5	0.1	1	0	0
Fig. 2f	0.56	0.1	1	0.05	0.5	0.1	1	0	0
Fig. 3a	0.65	0.6	1.45	0.05	0.5	0.2	0.2	0	0
Fig. 3b	0.6	0.6	1.35	0.05	0.5	0.2	0.2	0	0
Fig. 3c	0.5	0.6	1.25	0.01	0.25	0.02	0.2	0	0
Fig. 4a	4.575	0.5	6.2	1	1	0.02	0.2	0.40	0
Fig. 4b	4.5875	0.5	6.2	1	1	0.02	0.2	0.40	0
Fig. 4c	4.5975	0.5	6.2	1	1	0.02	0.2	0.40	0
Fig. 4d	4.5775	0.5	6.2	1	1	0.02	0.2	0	0.20
Fig. 4e	4.5825	0.5	6.2	1	1	0.02	0.2	0	0.20
Fig. 4f	4.5925	0.5	6.2	1	1	0.02	0.2	0	0.20
Fig. 4g	4.5775	0.5	6.2	1	1	0.02	0.2	0.30	0.03
Fig. 4h	4.4875	0.5	6.2	1	1	0.02	0.2	0.30	0.03

Fig. 4i	4.5975	0.5	6.2	1	1	0.02	0.2	0.30	0.03

Fig. 2 demonstrates the spatial patterns induced by pure Turing instability undergo two significant transitions as the value of parameter *R* increases. The first transition progresses from hot spot patterns through stripe-spot hybrid states to stripe patterns, while the second evolves from stripe patterns via hybrid states into fully cold spot patterns. Fig 3 shows the occurrence of non-Turing patterns. Fig. 3a and 3b display the spiral patches, and it is found that increasing the values of *R* and *S* can enhance the curl degree of the spirals. Fig. 3c displays the circle patches, and the pattern is alternating between regular and irregular rings.

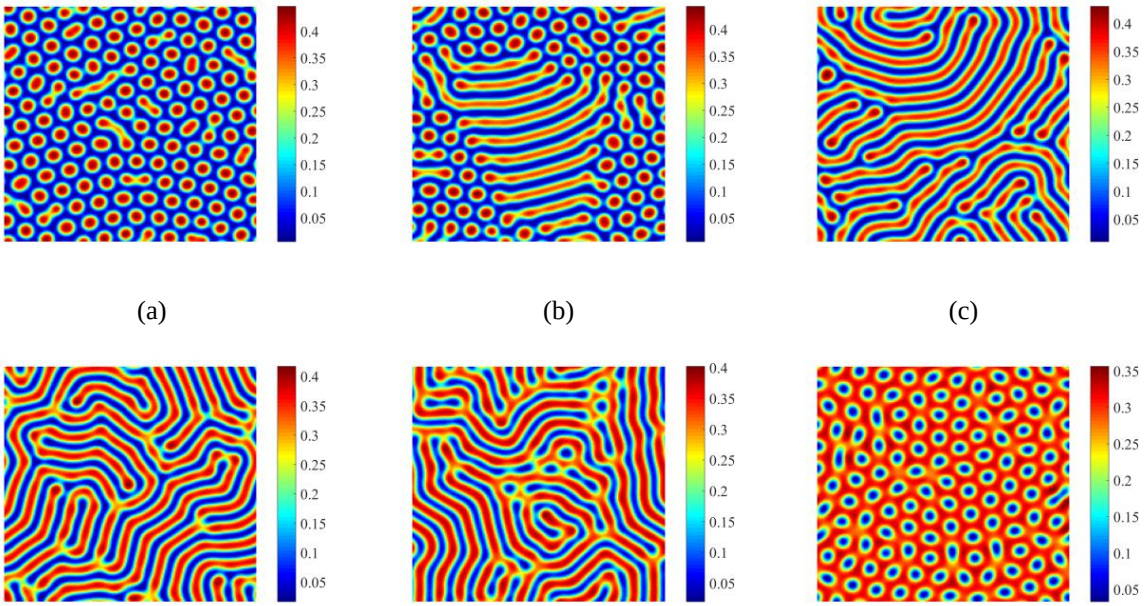

Fig. 2 Transition of spots and stripes Turing patterns with the increase of *R*.

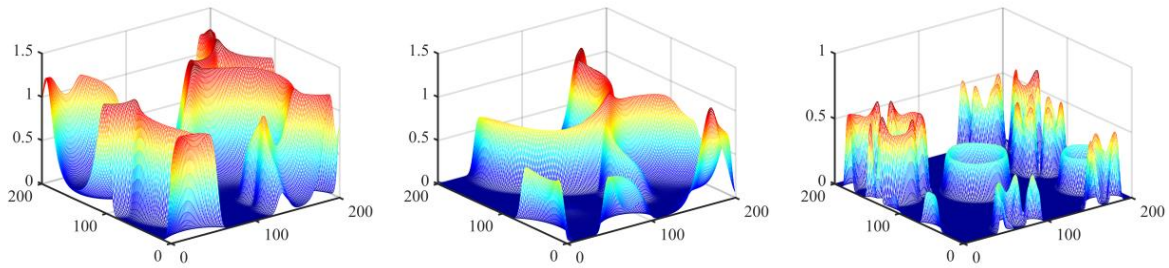

Fig. 3 Occurrence of non-Turing patterns with spirals and circles.

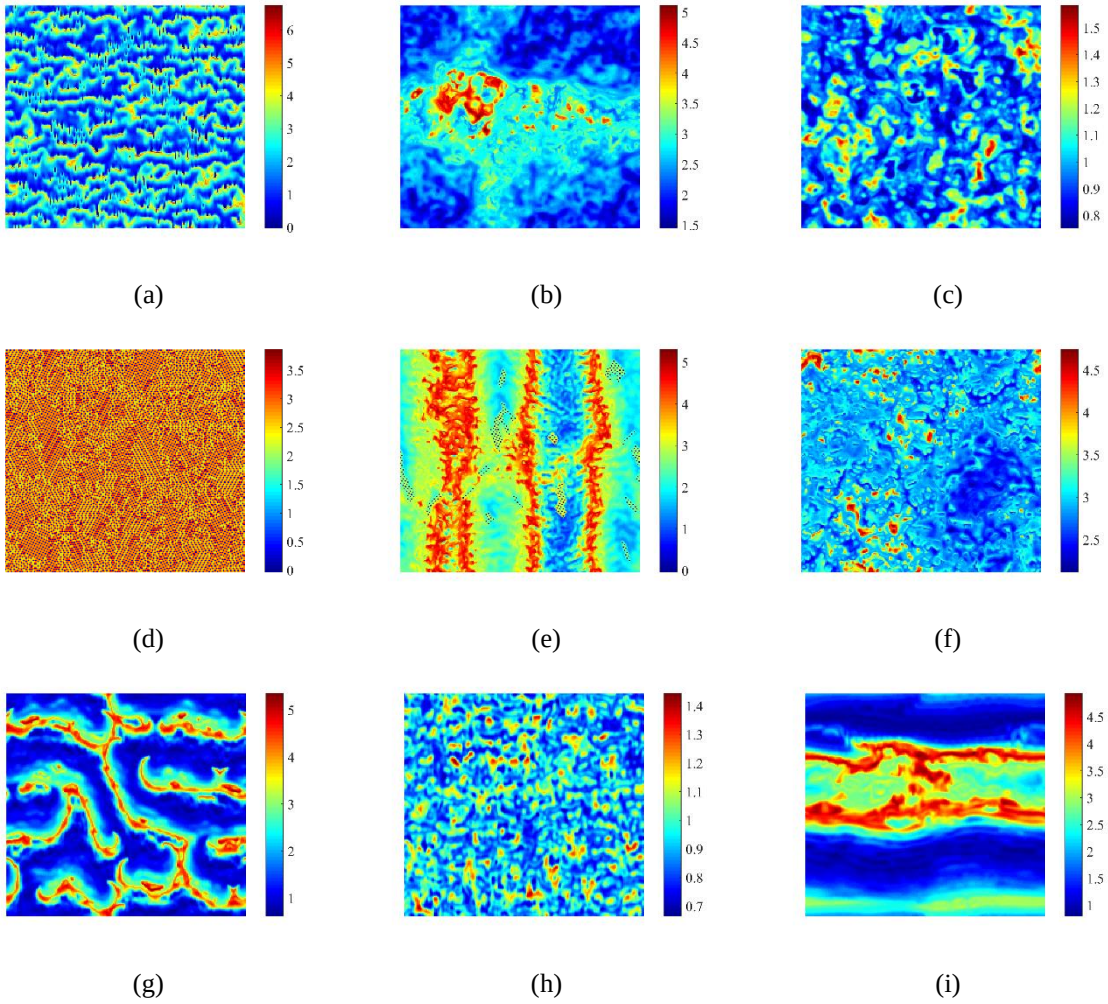

Fig. 4 Complex patterns and pattern transition on the route to chaos.

Notice that the patterns in Figs. 2 and 3 are formed without the effect of migration. Fig. 4 demonstrates the complex pattern self-organization and pattern transition on the route to chaos induced by the bifurcation, under the impact of migration. Three cases are shown, prey migration without predator migration (Fig. 4a-c), predator migration without prey migration (Fig. 4d-f), predator and prey migration (Fig. 4g-i). We find the formation of banded, turbulent, irregular spot, spiral, stripe patterns, and etc. Here, notice that the migration will not inevitably lead to the formation of stripe or band patterns. With the variation of parameter R, the transition of patterns on the routes to chaos are really vary complicated. These results display the spatiotemporal complexity of the discrete system under the influence of diffusion and migration. And the quantitative analysis on the pattern formation and transition should be extended in the future research.

4. Conclusions

This study explores the pattern formation in a discrete predator-prey system with migration and diffusion. The analysis reveals that migration significantly enhances spatial coupling, influencing pattern formation and transition. Numerical simulations demonstrate diverse pattern formations, showing the complexity of the system. These results provide insights into spatiotemporal dynamics and highlight the role of migration in pattern self-organization.

References

[1] Wen M, Zhang G, Yan Y. Turing instability of a discrete competitive single diffusion-driven Lotka–Volterra model. Chaos, Solitons and Fractals, 2025, 194: 116146.

[2] Han X, Lei C. Stability, bifurcation analysis and pattern formation for a nonlinear discrete predator–prey system. Chaos, Solitons and Fractals, 2023: 173: 113710.

[3] Kondo S, Miura T. Reaction-diffusion model as a framework for understanding biological pattern formation. Science, 2010, 329(5999): 1616.

[4] Mehdi R, Wu R, Hammouch Z. Chaotic bifurcation dynamics in predator–prey interactions with logistic growth and Holling type-II response. Alexandria Engineering Journal, 2025, 115: 119-130.

[5] Salman S M , Han R. Spatiotemporal patterns in a space–time discrete SIRS epidemic model with self- and cross-diffusion. International Journal of Bifurcation & Chaos, 2024, 34(8): 637-655.

[6] Huang T, Zhang H, Yang H. Spatiotemporal complexity of a discrete space-time predator− prey system with self-and cross-diffusion. Applied Mathematical Modelling, 2017, 47: 637-655.

[7] Sun G-Q, Jin Z, Liu Q-X, Li L. Dynamical complexity of a spatial predator–prey model with migration. Ecological Modelling, 2008, 219(1-2): 248-255.

[8] Bi Z, Liu S, Ouyang M, et al. Pattern dynamics analysis of spatial fractional predator-prey system with fear factor and refuge. Nonlinear dynamics, 2023, 111: 10653–10676.

[9] Huang T, Zhang H. Bifurcation, chaos and pattern formation in a space-and time-discrete predator–prey system. Chaos, Solitons & Fractals, 2016, 91: 92-107.

[10] Liu X, Xiao D. Complex dynamic behaviors of a discrete-time predator–prey system. Chaos, Solitons & Fractals, 2007, 32(1): 80-94.

[11] Jing Z, Yang J. Bifurcation and chaos in discrete-time predator–prey system. Chaos, Solitons & Fractals, 2006, 27(1): 259-277.

[12] Huang T, Zhang H, Yang H, et al. Complex patterns in a space-and time-discrete predator-prey model with Beddington-DeAngelis functional response. Communications in Nonlinear Science and Numerical Simulation, 2017, 43: 182-199.